Supporting Information

Poly(3-hexylthiophene)-based non-fullerene solar cell achieves high photovoltaic performance with small energy loss

*Feng Liu, Jianyun Zhang, Zichun Zhou, Jianqi Zhang, Zhixiang Wei and Xiaozhang Zhu**

Materials

All the reactions dealing with air- or moisture-sensitive compounds were carried out in a dry reaction vessel under a positive pressure of nitrogen. Unless otherwise stated, starting materials were obtained from Adamas, Aldrich, and J&K and were used without any further purification. Toluene was distilled over Na/benzophenone prior to use. Dioctyl-4,4'-(4,4,9,9-tetrakis(4-hexylphenyl)-4,9-dihydro-s-indaceno[1,2-*b*:5,6-*b*']dithiophene-2,7-diyl)bis(6-formylthieno[3,4-*b*]thiophene-2-carboxylate) was prepared according to the published procedures (F. Liu, Z. Zhou, C. Zhang, T. Vergote. H. Fan, F. Liu, X. Zhu, *J. Am. Chem. Soc.* 2016, **138**, 15523.). P3HT was purchased from 1-Material Chem-scitech Inc. and used as received.

Measurements

Hydrogen nuclear magnetic resonance (^{1}H NMR) and carbon nuclear magnetic resonance (^{13}C NMR) spectra were measured on BRUKER DMX 400 spectrometers. Chemical shifts for hydrogens are reported in parts per million (ppm, δ scale) downfield from tetramethylsilane and are referenced to the residual protons in the NMR solvent ($CDCl_3$: δ 7.26). ^{13}C NMR spectra were recorded at 100 MHz. Chemical shifts for carbons are reported in parts per million (ppm, δ scale) downfield from tetramethylsilane and are referenced to the carbon resonance of the solvent ($CDCl_3$: δ 77.0). The data are presented as follows: chemical shift, multiplicity (s = singlet, d = doublet, t = triplet, m = multiplet and/or multiple resonances, br = broad), coupling constant in Hertz (Hz), and integration. MALDI-TOF measurements were performed on an Applied Biosystems 4700 Proteomics Analyzer. Elemental analyses were measured on a Carlo Erba 1106 elemental analyzer. UV-vis spectra were recorded on a JASCO V-570 spectrometer. Cyclic voltammetry (CV) measurements were carried out on a CHI640C analyzer in a conventional three-electrode cell setup with glassy-carbon electrode as the working electrode, a platinum wire as the counter electrode, Ag/Ag^+ as the reference electrode and calibrated with ferrocene/ferrocenium (Fc/Fc^+) as an external potential marker in anhydrous CH_2Cl_2 solution containing 0.1 M tetrabutylammonium perchlorate (TBAP) as a supporting electrolyte under a nitrogen atmosphere at room temperature. All potentials were corrected against Fc/Fc$^+$. CV was measured with a scan rate of 100 mV/s. Thermogravimetric analysis (TGA) was performed on a Shimadzu DTG 60 instrument at a heating rate of 10 °C min^{-1} under a N_2 atmosphere with runs recorded from room temperature to 550 °C. Atomic force microscopy (AFM) images of the thin films were obtained on a NanoscopeIIIa AFM (Digital Instruments) operating in tapping mode. 2D-GIWAXS were conducted on a Xeuss SAXS/WAXS system with X-ray wavelength of 1.5418 Å. The film samples were irradiated at a fixed angle of 0.2^o .

Fabrication of organic solar cells

PSCs were fabricated with the structures ITO/PEDOT:PSS/P3HT:ATT-3/Ca/Al. The devices were fabricated using ITO-coated glass substrates (15 Ω sq^{-1}), which were cleaned with deionized water, acetone, and isopropyl alcohol in successive 20 min sonication steps applying a final 20 min oxygen plasma treatment to eliminate any remaining organic component. A thin layer (ca. 30 nm) of PEDOT:PSS was first spin-coated on the pre-cleaned ITO-coated glass substrates at 3000 rpm. After baking at 150 °C for 15 min under ambient conditions, the substrates were then transferred into a nitrogen-filled glovebox. The active layer was spin-coated on PEDOT:PSS substrate at 3000 rpm for 60 s from 1.11 ml of chloroform solution containing P3HT (10 mg) and ATT-3 (8 mg). The active layer (≈ 70 nm) was annealed at 130 °C for 10 min on a digitally controlled hot plate. Thin layer of Ca (20 nm) was deposited as the electron transport interlayer, and Al (100 nm) were deposited as the top electrode. The active area of the device was *ca.* 4 mm^2.

Device Characterization

The current density–voltage (*J–V*) characteristics of unencapsulated photovoltaic devices were measured under N_2 using a Keithley 2400 source meter. A 300 W xenon arc solar simulator (Oriel) with an AM 1.5 global filter operated at 100 mW cm^{-2} was used to simulate the AM 1.5G solar irradiation. The illumination intensity was corrected by using a silicon photodiode with a protective KG5 filter calibrated by the National Renewable Energy Laboratory (NREL). The external quantum efficiency (EQE) was performed using certified IPCE equipment (Zolix Instruments, Inc, SolarCellScan100).

SCLC Mobility Measurements

Space charge-limited currents were tested in electron-only devices with a configuration of ITO/ZnO/ P3HT:ATT-3/Al and hole-only devices with a configuration of ITO/PEDOT:PSS/ P3HT:ATT-3/MoO_3/Al. The devices were prepared following the same procedure described in the experimental section for photovoltaic devices, except for the metal electrode. The mobilities were determined by fitting the dark current to the model of a single carrier SCLC current with field dependent mobility, which is described as

$$J = \frac{9\varepsilon_0\varepsilon_r\mu_0 V^2}{8L^3} \qquad (1)$$

Where J is the current, μ_0 is the zero-field mobility, ε_0 is the permittivity of free space, ε_r is the relative permittivity of the material, V is the effective voltage, and L is the thickness of the active layer.

Scheme S1. The synthesis route of ATT-3[a].

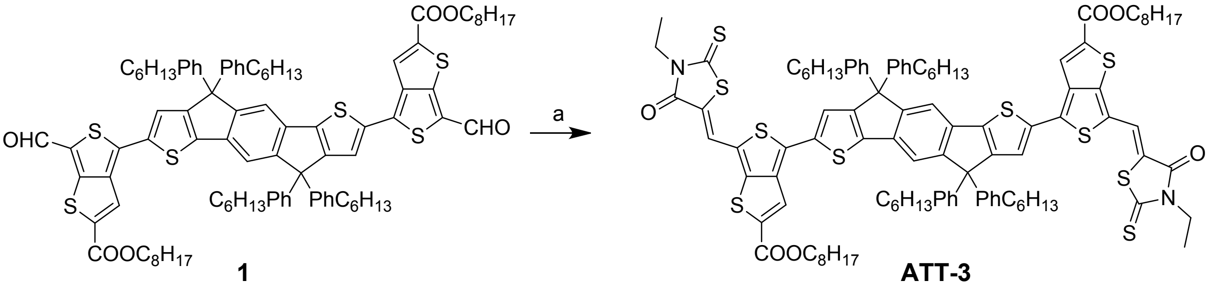

[a]The reaction condition: 3-ethyl-2-thioxothiazolidin-4-one, *β*-alanine, $ClCH_2CH_2Cl/C_2H_5OH$, reflux.

Synthesis of dioctyl 4,4'-(4,4,9,9-tetrakis(4-hexylphenyl)-4,9-dihydro-*s*-indaceno[1,2-*b*:5,6-*b*']dithiophene-2,7-diyl)bis(6-((3-ethyl-4-oxo-2-thioxothiazolidin-5-ylidene)methyl)thieno[3,4-*b*]thiophene-2-carboxylate) (ATT-3): Compound **1** (155.0 mg, 0.1 mmol) and *β*-alanine (1.8 mg, 0.02 mmol) were dissolved in $ClCH_2CH_2Cl/C_2H_5OH$ (6 ml/3 ml). 3-ethyl-2-thioxothiazolidin-4-one (161.0 mg, 1.0 mmol) was then added and the mixture stirred and refluxed overnight. The resulting mixture was extracted with chloroform, washed with water, and dried over $MgSO_4$. After removal the solvent, the crude product was purified on a silica-gel column chromatography to give 128 mg of compound **ATT-3** in 70% yield as a dark solid. ^1H NMR (400 MHz, $CDCl_3$): δ 0.87 (m, 18H), 1.26–1.53 (m, 50H), 1.57−1.65 (m, 8H), 1.76−1.81 (m, 4H), 2.59 (t, ^3J = 8.0 Hz, 8H), 4.20 (m, 4H), 4.36 (t, ^3J = 6.8 Hz, 4H), 7.13 (d, ^3J = 8.0 Hz, 8H), 7.21 (d, ^3J = 8.4 Hz, 8H), 7.37 (s, 2H), 7.50 (s, 2H), 7.87 (s, 2H), 8.02 (s, 2H); ^{13}C NMR (100 MHz, $CDCl_3$): δ 191.04, 167.02, 162.08, 157.92, 154.29, 147.88, 144.50, 142.08, 140.87, 140.77, 140.14, 138.00, 137.51, 135.36, 128.67, 127.78, 123.79, 122.60, 121.83, 121.55, 119.39, 117.98, 77.32, 77.00, 76.68, 66.26, 63.22, 40.04, 35.59, 31.77, 31.70, 31.33, 29.15, 28.61, 25.88, 22.64, 22.59, 14.09, 12.29; HRMS (MALDI-TOF) Calcd for $C_{106}H_{120}N_2O_6S_{10}$ $[M]^+$: 1836.6353; found, 1836.6339; Anal. Calcd for $C_{106}H_{120}N_2O_6S_{10}$ (%): C, 69.24; H, 6.58; N, 1.52; Found (%): C, 69.28; H, 6.63; N, 1.46.

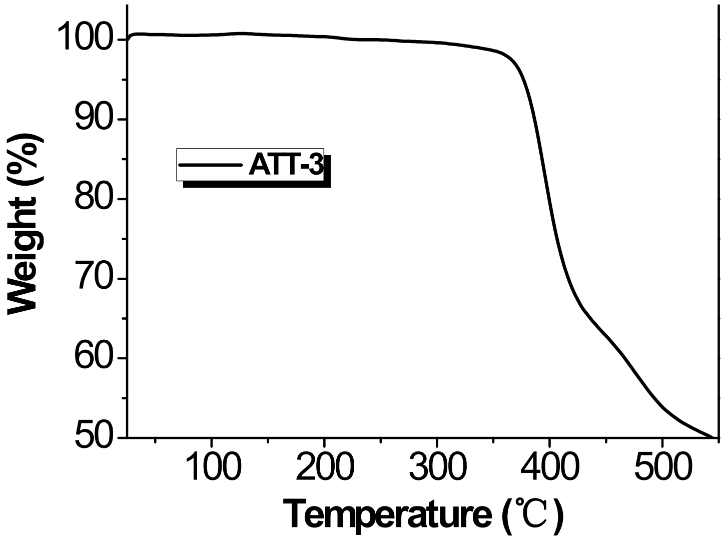

Fig. S1 Thermal gravimetric analysis (TGA) curves of compound **ATT-3**.

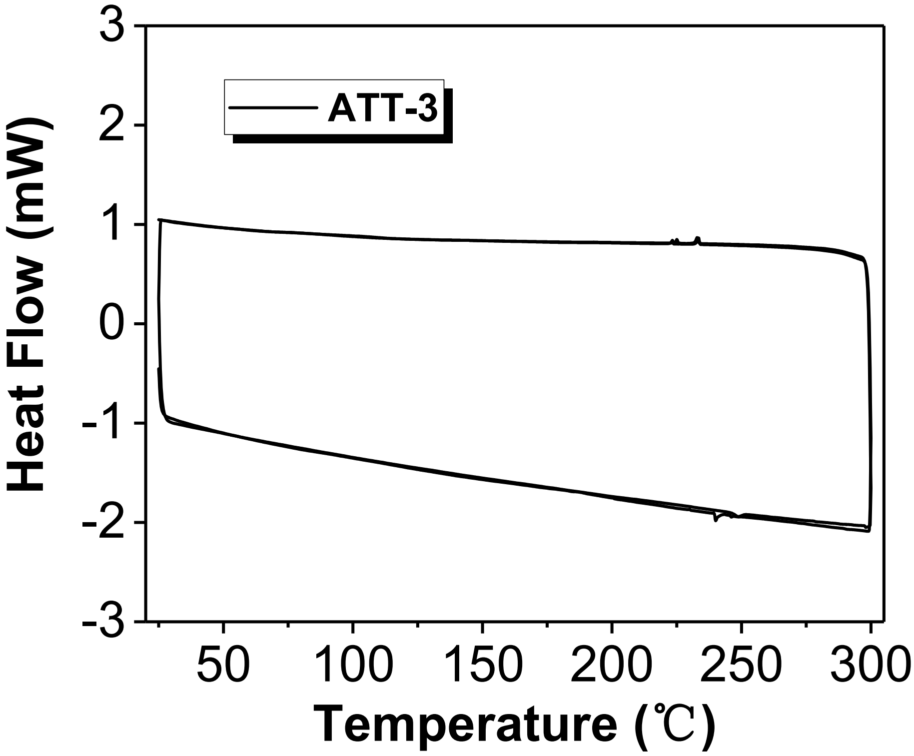

Fig. S2 Differential scanning calorimetry (DSC) curves of powders of ATT-3.

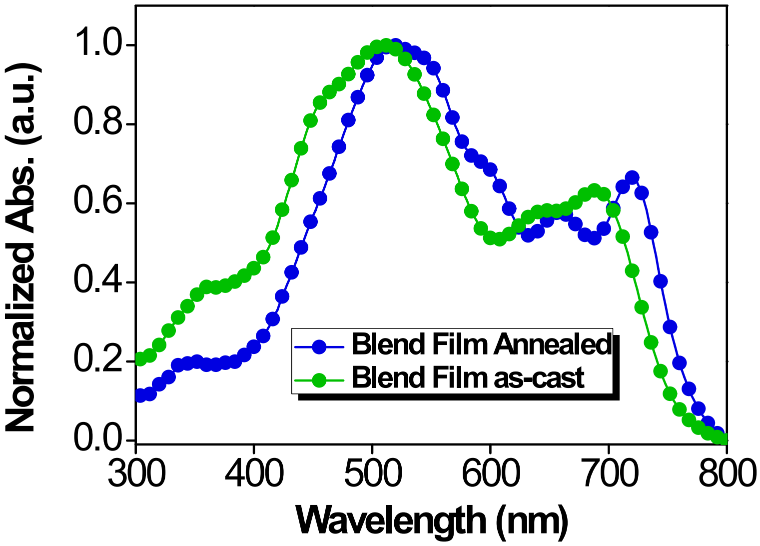

Fig. S3 The normalized as-cast and annealed blend film absorption spectrum.

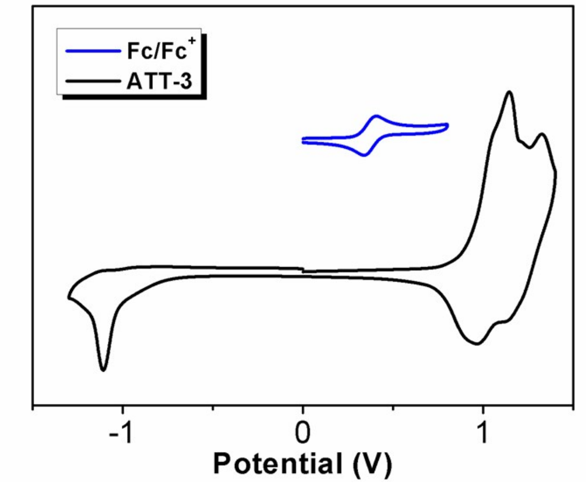

Fig. S4 Cyclic voltammogram of **ATT-3** film deposited on glass carbon electrode in 0.1 M *n*-Bu_4NClO_4 acetonitrile solution at a scan rate of 10 mV s^{-1}.

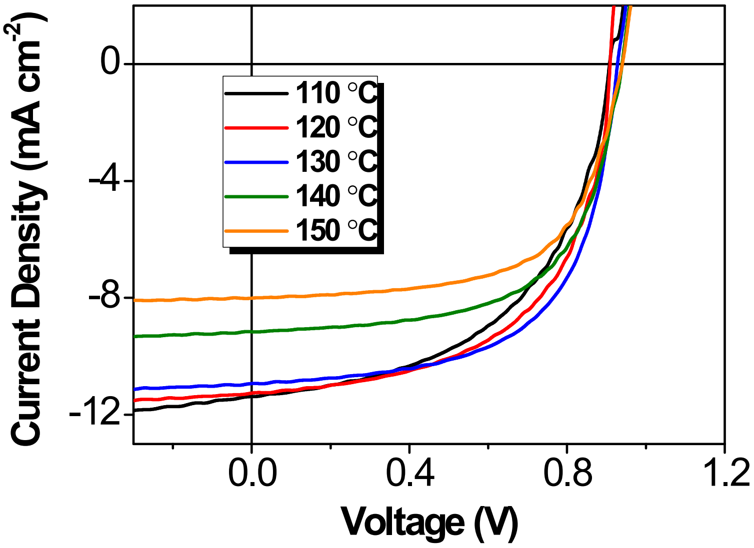

Fig. S5 *J*-*V* curves of P3HT:ATT-3 (1:0.8, w/w) blend film with different thermal annealing temperature.

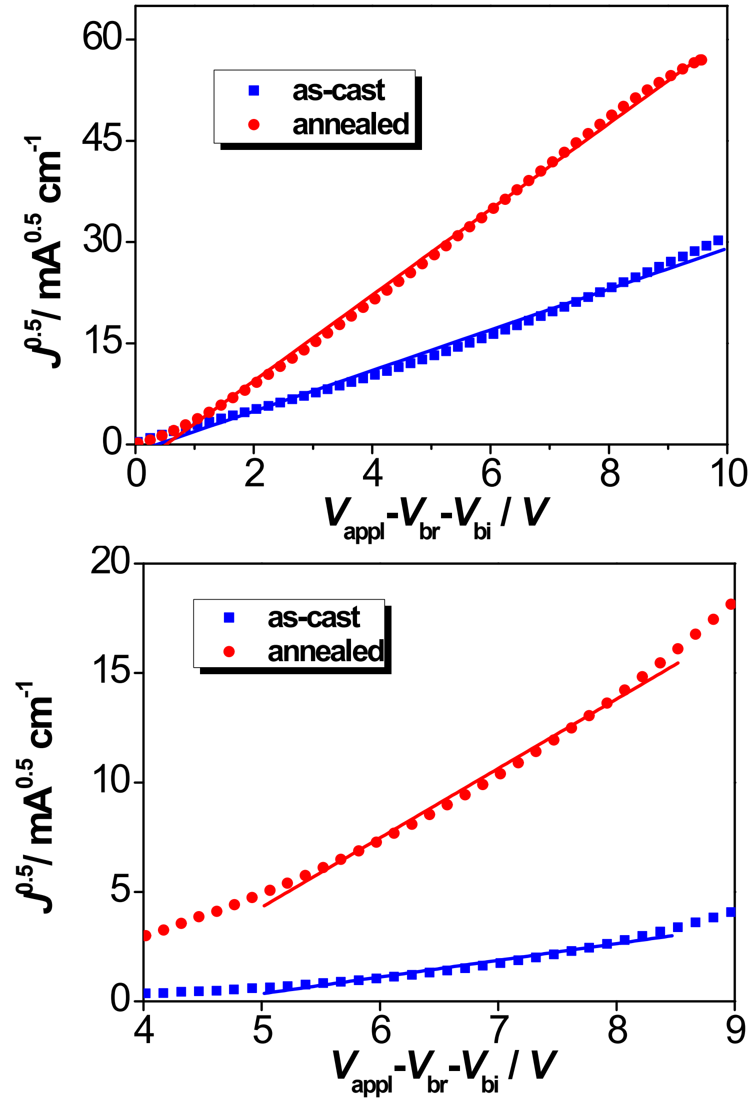

Fig. S6 The hole mobility (up) and electron mobility (down) of P3HT:ATT-3 as-cast or thermal annealed blend films at their best OSC device characters measured by SCLC method.

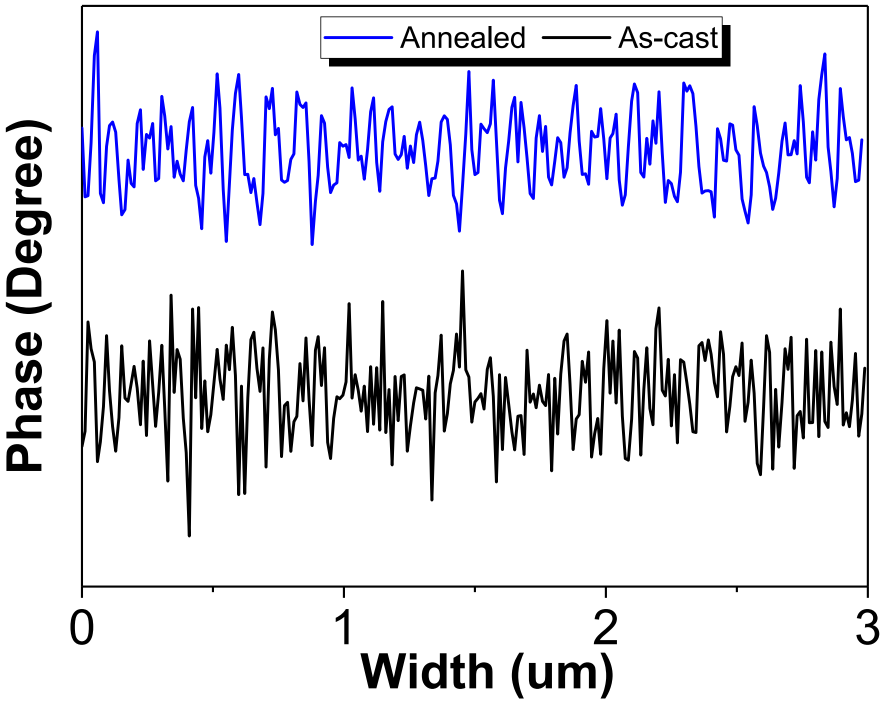

Fig. S7 AFM section curves of P3HT:ATT-3 blend film without thermal annealing (black line) and annealed at 130 °C (blue line).

Table S1 The photovoltaic performance of P3HT:ATT-3 blend films with different thermal annealing temperatures.

D/A ratio [w/w]	Thermal Anneling [°C]	V_{oc} [V]	J_{sc} [mA/cm^2]	FF [%]	PCE [%]	
					Best	Ave.
1:0.8	110	0.907	11.42	53.0	5.49	5.31
1:0.8	120	0.909	11.26	57.9	5.93	5.82
1:0.8	130	0.927	10.93	61.8	6.26	6.11
1:0.8	140	0.939	9.16	62.1	5.34	5.25
1:0.8	150	0.940	8.02	62.9	4.75	4.62

ATT-3

^{1}H NMR

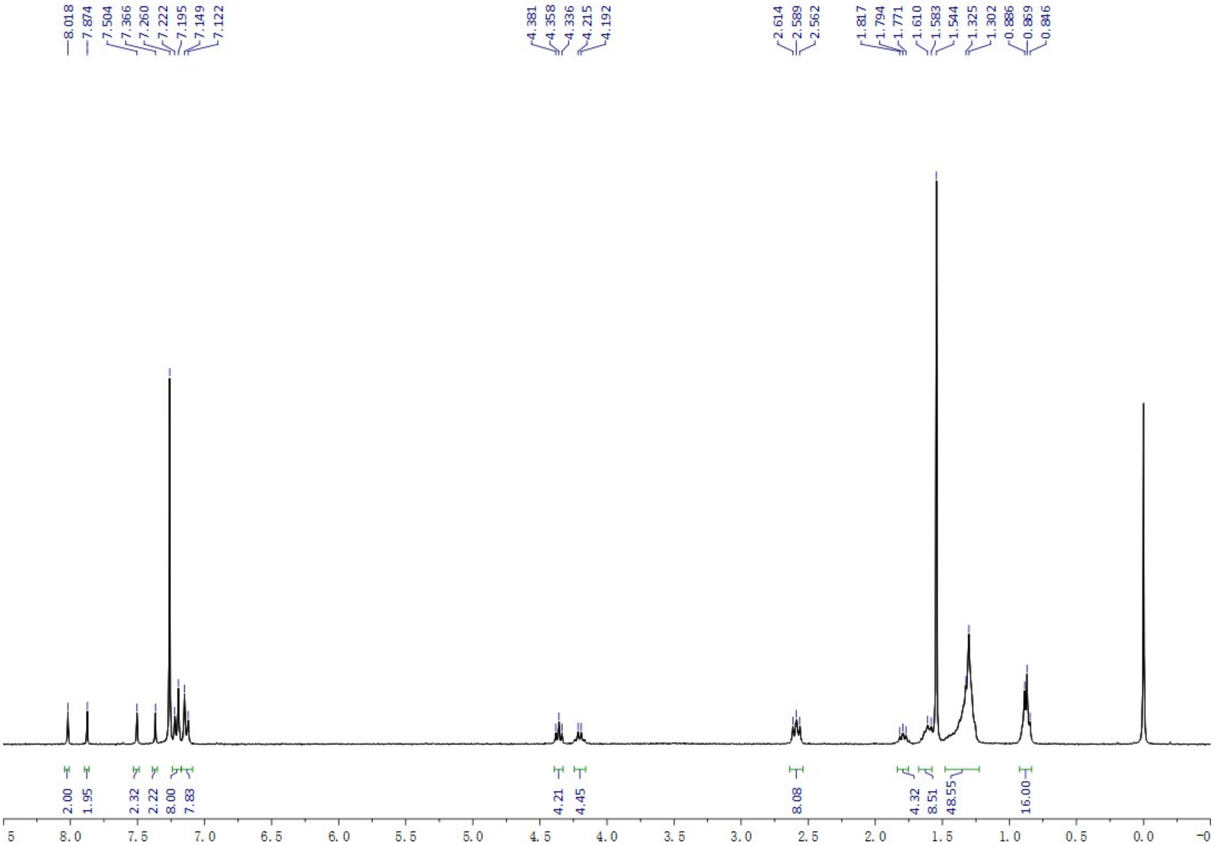

^{13}C NMR